Journal of Cellular Biochemistry 99:256–268 (2006)

Differential Expression of Proteins in Kidney, Eye, Aorta, and Serum of Diabetic and Non-Diabetic Rats

William C. Cho,[1]* Tai-Tung Yip,[2] Wai-Shing Chung,[1] Albert W. Leung,[3] Christopher H. Cheng,[4] and Kevin K. Yue[1]

[1]School of Chinese Medicine, Hong Kong Baptist University, Hong Kong
[2]Ciphergen Biosystems, Inc., Fremont, California
[3]School of Chinese Medicine and Health Care, CU-TWCC, Hong Kong
[4]Department of Biochemistry, The Chinese University of Hong Kong, Hong Kong

Abstract Diabetes mellitus (DM) is a chronic progressive disease that often results in microvascular and macrovascular complications, yet its pathogenesis is not clear. Automated proteomic technology, coupled with powerful bioinformatics and statistical tools, can provide new insights into the molecular alterations implicated in DM. Following our previous findings of redox changes in the eye and aorta of diabetic rats, as well as the activities of different antioxidant enzymes during the development of DM, this study is further launched to find potential biomarkers by comparing the serum and tissue samples of 26 diabetic rats (8 weeks after streptozotocin [STZ] administration) with 29 normal controls using surface enhanced laser desorption/ionization time-of-flight mass spectrometry (SELDI-TOF MS) technology. Eight potential biomarkers were found in the serum, one potential biomarker was found in the kidney and eye, respectively, whereas three potential biomarkers were discovered in the aorta. One of the serum biomarker candidates was found to match the C-reactive protein (CRP) in the Swiss-Prot knowledgebase. Further validation has been conducted by ELISA kit to confirm the role of CRP during the development of DM. To conclude, the increased level of CRP in diabetic serum demonstrated in this study indicates that the development of DM is associated with inflammation. This is also the first report demonstrating that some potential lysate biomarkers in the kidney, eye, and aorta may be involved in the development of diabetes and its complications. Further identification and evaluation of these potential biomarkers will help unravel the underlying mechanisms of the disease. J. Cell. Biochem. 99: 256–268, 2006.

Key words: diabetes mellitus; diabetic complications; proteomics; SELDI-TOF MS

Diabetes mellitus (DM) is one of the top five global leading causes of death. In the year 2000, the excess global mortality attributable to diabetes and its late complications was estimated to be 2.9 million deaths, equivalent to 5.2% of all deaths [Roglic et al., 2005]. Despite decades of intensive research into its pathogenesis, the triggering factors and underlying mechanism behind the development of DM and its complications remain largely unknown.

Type 1 diabetes has highest incidence in children and adolescents. It is characterized by pancreatic β-cell destruction, which usually leads to an absolute deficiency of insulin. Around 90–95% of DM are type 2 diabetes which is characterized by insulin resistance as insulin-receptor in body cells do not bind and response appropriately when insulin is present. Severe complications can be resulted from latent type 2 diabetes with the vasculature exposed to an unfavorable internal environment arising from hypertension, dyslipidemia, inflammation, and impaired fibrinolysis [Hanson et al., 2002].

Abbreviations used: CHAPS, 3-[3-(Cholamidopropyl) dimethylammonio]-1-proanesulfonate; CRP, C-reactive protein; DM, diabetes mellitus; DN, diabetic nephropathy; DR, diabetic retinopathy; IMAC3-Cu, immobilized metal affinity capture-copper; PCA, principal components analysis; ROC, receiver-operator characteristic; SD, Sprague–Dawley; SELDI-TOF MS, surface-enhanced laser desorption/ionization time-of-flight mass spectrometry; STZ, streptozotocin; TIC, total ion current.

Grant sponsor: Hong Kong Baptist University Faculty Research Grant.

*Correspondence to: William C. Cho, PhD, Room 1327, 13/F, Block R, Queen Elizabeth Hospital, 30 Gascoigne Road, Kowloon, Hong Kong. E-mail: williamcscho@gmail.com

Received 20 October 2005; Accepted 23 February 2006
DOI 10.1002/jcb.20923

Patient with DM may experience a series of intractable long-term complications. Hyperglycemia induced adverse effects on various systemic systems and sensory organs of the body, resulting in heart failure, stroke, claudication, retinopathy, nephropathy, neuropathy, and skin dysfunction. Most of these complications are progressive and they usually develop over years. The longer the patient has been suffering from DM, the more likely that complications will arise.

Diabetic nephropathy (DN) is one of the main causes of morbidity and mortality in patients with DM [Phillips and Molitch, 2002]. Approximately 40% of type 2 DM patients will develop diabetic kidney disease [Lewis and Lewis, 2003]. Diabetic retinopathy (DR) is also a major complication of DM and is a leading cause of acquired blindness. Blood-retinal barrier breakdown is a hallmark of this microvascular disease and around 85% of all diabetics eventually develop retinopathy [Tewari and Venkatesh, 2004]. On the other hand, cardiovascular impact accounts for the greatest morbidity and mortality associated with DM, such as coronary atherosclerosis, hypertension, and cardiomyopathy. Macrovascular diseases are two to six times more common among people with DM, such as coronary artery disease, peripheral artery disease, and stroke [Varughese et al., 2005].

Hyperglycemia is the primary cause of diabetic complications, but the underlying mechanisms are not clear. During the past decade, proteomics has been extensively applied to various fields of biological and medical research. While many investigators have used surface-enhanced laser desorption/ionization time-of-flight mass spectrometry (SELDI-TOF MS) technology to study malignancies [Yip and Lomas, 2002], proteomic profiling of DM is still in its infancy. Proteomics is a powerful platform for investigating protein expression profiles and their modifications in response to specific physiological or pathophysiological conditions in biological systems. It can be particularly useful for the identification of molecular alterations implicated in diabetes [Cho et al., 2005].

We have previously demonstrated that redox status and oxidative stress occurred in the eye and aorta but not in the kidney of diabetic rats 8 weeks after streptozotocin (STZ) injection, and the onset of oxidative stress was preceded by a depletion of glutathione in the tissues [Yue et al., 2003]. Moreover, we also demonstrated that different tissues employed different antioxidant enzymes in their defense against oxidative stress during the development of diabetes [Yue et al., 2005]. The present study focuses on the protein disregulation in the sera and tissues of diabetic rats 8 weeks after STZ injection by proteinchip profiling analysis. In this study, high-throughput MS and bioinformatic technologies were applied to find potential biomarkers so as to enhance a better understanding of diabetes and its complications, as well as to explore the complexity of the disease mechanisms.

MATERIALS AND METHODS

Experimental Animals

Wild-type outbreed male Sprague–Dawley (SD) rats (250–300 g) were provided by the Laboratory Animal Service Centre (The Chinese University of Hong Kong). Experimental DM was induced by double intraperitoneal injection of STZ as previously described [Yue et al., 2003]. Briefly, the animals were injected with STZ (40 mg/kg) on 2 consecutive days [Arulmozhi et al., 2004]. At the 4th and 8th week after STZ injection, body weight was measured on a standardized digital scale while venous blood samples were collected from the tails of overnight fasted rats in order to measure their corresponding serum glucose level by the Glucose Diagnostic Kit (Sigma, St Louis, MO), 26 rats with confirmed serum glucose level $>$ 300 mg/dl at both time points were used as the diabetic rat model. Twenty-nine age-matched normal male SD rats injected with the same amount of 0.1 M sodium citrate were used as the control group. Comparing to the non-diabetic rats, the mean body weight of the diabetic rats was significantly lower at the 4th week (445 ± 28 g vs. 282 ± 93 g, $P < 0.001$) and 8th week (528 ± 51 g vs. 247 ± 32 g, $P < 0.001$) after STZ administration. All the animals were housed (three to four per cage) under a daily cycle of 12 h light and 12 h darkness, supplied with food and water ad libitum and then used 8 weeks after the injection. All rats were treated in compliance with the approved guidelines for animal experiments established by the Hong Kong Baptist University Animal Research Committee.

Sampling of Sera and Tissues

Animals were deprived of food for 8–10 h and killed by cervical dislocation on the day of

sacrifice. Blood samples were collected together with excision of the whole kidney, eye (anterior segment of the eye, lens, and optical nerve were discarded), and descending aorta tissues.

Each blood sample was allowed to clot and centrifuged at 1,500*g* for 10 min. Sera were collected, aliquoted and kept frozen at −80°C. When the experiment was carried out, the serum samples were thawed and 20 μl of each sample was denatured by adding 30 μl of 50 mM Tris-HCl buffer containing 9 M urea and 2% 3-[3-(Cholamidopropyl) dimethylammonio]-1-proanesulfonate (CHAPS) at pH 9.

Each tissue sample was rinsed with ice-cold phosphate buffered saline (137 mM NaCl, 2.7 mM KCl, 10 mM Na_2HPO_4, 1.8 mM KH_2PO_4, pH 7.4) and blotted dry, then frozen immediately in liquid nitrogen and stored at −80°C. When the experiment was carried out, the tissue samples were homogenized in a chilled mechanical homogenizer at 4°C using 20 strokes for each tissue sample. The mixture was then centrifuged at 12,000*g* for 15 min at 4°C. The supernatant was taken out and isopropanol (1.5 ml per 50 mg of tissue) was added. The precipitated protein/peptide was then washed with 0.3 M guanidine hydrochloride/95% ethanol (2 ml per 50 mg of tissue). After washing, 2 ml of 100% ethanol was added and the resulting mixture was centrifuged. Finally, 150 μl 6 M guanidine thiocyanate, 1% octyl-β-D-glucopyranoside and 350 μl 9 M urea, 2% CHAPS in 50 mM Tris-HCl at pH 9 were added to the protein pellet for dissolution.

After the above preparation procedures, the protein/peptide in each serum and tissue sample was fractionated in an anion exchange Ciphergen Q HyperD F 96-well filter plate. The protein/peptide bound by the ion exchange beads was eluted by a pH 9 elution buffer, followed subsequently by buffers at pH 7, pH 5, pH 4, pH 3, and finally by an organic buffer containing isopropanol, acetonitrile, and trifluoacetic acid as previously described [Cho et al., 2004; Yip et al., 2005].

SELDI-TOF MS Profiling

All fractionation and profiling steps were performed on the Biomek 2000 Robotic Station (Beckman Coulter, Inc., Fullerton, CA) and Aquarius (Tecan Trading AG, Mannedorf, Switzerland). These integrated robots aid automated high-throughput proteinchip profiling by conducting sample loading and washing steps in a highly reproducible manner.

Each serum (n = 55) and lysate (n = 55 for each type of tissue) sample was profiled in duplicate on two types of proteinchip arrays (Ciphergen Biosystems, Inc., Fremont, CA), weak cationic exchange and immobilized metal affinity capture-copper (IMAC3-Cu), using different binding conditions for each array type as previously described [Cho et al., 2004]. The arrays were read in a proteinchip reader PBS IIc (Ciphergen Biosystems, Inc.) with mass deflection at 1.5 kDa and time-lag focusing. The acquisition range was set to 0–200 kDa and the instrument has a mass accuracy of 0.1% when properly calibrated, which was performed with the all-in-one peptide standard chip (seven peptide calibrants, 1–7 kDa, Ciphergen Biosystems, Inc.). The parameters used for spectral preprocessing and peak selection were: baseline subtraction, both the smoothing before fitting baseline and the automatic fitting width options selected (with a window of 25 data points for the former); filtering, variable width moving average filter of 0.2 times expected peak width; noise estimation: to start from 1.5 kDa; normalization by total ion current (TIC), to start from 1.5 kDa; peak detection, to start from 2 kDa and by centroid mass. Outlier spectra were excluded from further analysis if the normalization factor exceeded 2 standard deviations above the mean normalization factor. Two thousand six hundred and forty proteinchip spots on 330 chips of each type of proteinchip array were used, with the controls randomized and run concurrently with the disease samples on the same chip. Variability analyses were performed in a spot to spot and chip to chip fashion for both the IMAC3-Cu(II) and week cationic exchange chips as previously described. The chip-to-chip and spot-to-spot coefficient of variation were found to be 1–16% and 1–14%, respectively [Yip et al., 2005]. These variations were within 20% of other quality control study [Hong et al., 2005].

Bioinformatics and Statistical Analysis

CiphergenExpress Biomarker Analysis System (Ciphergen Biosystems, Inc.) was used to analyze all the spectra in this study. Baseline subtraction was first performed on individual spectra to eliminate systematic biases such as those generated by the energy absorbing molecules and "flatten" the spectra. Baseline corrected spectra were then normalized against each

other by TIC, which is defined as the sum of all the intensity values of a spectrum. The normalization process involved computing the TIC of each spectrum, and scaling the spectrum so that its new TIC equaled the collective mean TIC. Since TIC is a measure of the protein concentration (or other ionizable substances) of the sample, this in effect normalized all the spectra to the same sample concentration.

Peak detection was next performed on the normalized spectra and peaks of very similar m/z values across spectra were associated together into clusters which formed the initial pool of potential biomarkers. These two steps are automated by the Biomarker Wizard in Ciphergen ProteinChip Software 3.2.1 (Ciphergen Biosystems, Inc.). A signal-to-noise ratio >5 was used for the first pass peak detection and a signal-to-noise ratio >3 was used for the second pass. Additionally, a mass window of 0.3% of mass was specified as the maximum threshold for associating peaks together as one cluster, and a minimum peak threshold of 5% was chosen to reject clusters with too few peaks from the first pass peak detection. With these Biomarker Wizard parameters, a total of 948 peak clusters were obtained. A *P*-value was calculated for each of the peak clusters using the Mann–Whitney *U* test. Values of $P < 0.05$ were considered to be significant. The spectral region from 0–2 kDa is unreliable for both normalization and peak detection due to matrix interference and was therefore excluded in the analysis.

The Biomarker Analysis Module in CiphergenExpress Biomarker Analysis System was used to mine potential biomarkers while the supervised learning process of Biomarker Patterns Software 4.0.1 (Ciphergen Biosystems, Inc.) was used for cross-validation and bootstrapping for multiple testing to optimize the minimization of classification error.

The powerful analytical tools used in this study are broadly divided into univariate and multivariate. Univariate analytical tools included Mann–Whitney *U* test (non-parametric statistical significance test used to calculate a confidence interval for the median difference between two independent groups of sampled data [Whitney, 1997]), receiver-operator characteristic (ROC, plotting the dynamic relationship between sensitivity and specificity independent of disease prevalence [Nettleman, 1988]), scatter plot (displaying data points on a 2-D graph), Box and Whisker plot (displaying a statistical summary of the data values: median, 25–75 percentile quartiles and minimum to maximum value range); whereas multivariate analytical tools included principal components analysis (PCA, reducing the complexity of data and distinguishing sample clusters [Jayakar, 1980]), heat map (presentation of a dendrogram representing similarities in the expression patterns between the sample groups), classification and regression tree analysis (CART, predicting multiple potential biomarkers and cross-validation by applying the tree computed from learning sample to testing sample [Gribonval, 2005]).

Univariate analysis uncovers single potential biomarkers that can classify the sample groups by itself. In some cases univariate analysis alone is sufficient, but biological systems are usually complex and the disease can be caused by multiple factors. In those cases, multivariate analysis is needed to discover these factors for proper classification. In other words, if univariate analysis reveals individual biomarkers that can be positively identified and linked to the disease pathway, the CiphergenExpress Biomarker Analysis System would weigh over multivariate analytical tools such as the Biomarker Patterns Software.

Protein Matching

Protein matching was conducted via the Expert Protein Analysis System (Swiss Institute of Bioinformatics, Geneva, Switzerland), which is dedicated to the analysis of protein sequences and structures as well as 2-D gel. Using the TagIdent tool in the system, a list of proteins close to the molecular size and pI of our potential biomarkers can be generated, with molecular weight range within 0.1% and pI range within 0.1. Details (including the function of protein, domain structure, post-translational modifications, variants, etc.) of the matching protein can be retrieved by the Swiss-Prot protein knowledgebase in the system.

C-Reactive Protein (CRP) Measurement

The quantitative measurement of CRP in the rat serum was performed using the commercial Rat CRP ELISA Test Kit (Helica Biosystems, Inc., Fullerton, CA) with an intra-assay variability of 4–8%. Briefly, rat sera for testing were diluted to 1:4,000 and allowed to react with antibodies coated on specially treated

micro-wells. After appropriate incubation, the wells were washed to remove unreacted serum proteins, and an enzyme-labeled rabbit anti-rat CRP (conjugate) was then added to react with and tag the antigen-antibody complexes. Following another incubation period, the wells were washed again to remove unreacted conjugate. A urea peroxide substrate with tetramethylbenzidine as chromogen was added to initiate color development. Development of a blue color indicated a positive reaction while negative reactions appeared colorless or with a trace of blue. The reaction was interrupted with a stop solution that turned the blue positive reactions to yellow. Negative reactions remained colorless or with a hint of yellow. Color intensity (absorbance) was read at a wavelength of 450 nm on a spectrophotometer (Tecan Trading AG). Semi-quantification of absorbance was accomplished using a standard curve generated by measuring twofold dilutions of the standard provided.

RESULTS

Overview of Potential Biomarkers in the Serum and Tissue Lysates

By SELDI-TOF MS technology, 13 potential biomarkers were discovered in the serum and different organs of DM rats. Among them, eight biomarker candidates (at 3,507, 3,968, 5,165, 6,150, 11,612, 25,491, 47,736, and 76,433 Da) were found in the serum, one biomarker candidate (at 13,983 Da) in the kidney, one biomarker candidate (at 5,621 Da) in the eye, and three biomarker candidates (at 10,039, 10,803, and 11,077 Da) in the aorta (Table I).

Serum Protein Profile Alterations in Diabetic Rats

Comparing the serum proteinchip profiles of the 26 DM rats with those of the 29 normal controls, 532 peak clusters were found. Among which, 353 were statistically significant ($P < 0.05$). The top eight biomarker candidates were selected with the highest sensitivities ($\geq$86%) and specificities ($\geq$75%) to differentiate the diabetic samples from the controls. The representative peaks of interest were illustrated in Table I and Figure 1.

Protein Matching and Validation

These potential biomarkers have not yet been identified. As the first step discovery,

TABLE I. Potential Biomarkers for Diabetes Mellitus

	m/z	Peak intensity (mean ± SD)		Sensitivity (%)	Specificity (%)	Classification accuracy (%)	Change in DM	% of difference	*P*-value
	(Da)	Diabetes	Normal						
Serum	3,507	8.816 ± 2.382	2.968 ± 0.915	100	97	98	Increase	197	2.9E-10
	3,968	11.307 ± 6.145	2.047 ± 0.768	92	93	93	Increase	452	1.1E-8
	5,165	9.011 ± 3.565	1.069 ± 0.341	96	100	98	Increase	743	4.0E-9
	6,150	1.758 ± 0.692	0.873 ± 0.410	86	75	81	Increase	101	9.4E-7
	11,612	2.319 ± 0.499	0.973 ± 0.218	100	100	100	Increase	145	5.2E-9
	25,491	0.299 ± 0.053	0.175 ± 0.022	92	100	96	Increase	71	7.2E-8
	47,736	0.420 ± 0.131	0.162 ± 0.039	96	97	96	Increase	159	7.8E-8
	76,433	5.654 ± 1.052	4.009 ± 0.695	88	79	84	Increase	41	4.8E-5
Kidney	13,983	2.508 ± 0.734	1.258 ± 0.324	92	93	93	Increase	99	2.2E-9
Eye	5,621	1.023 ± 0.419	2.655 ± 1.323	88	86	87	Decrease	61	3.6E-5
Aorta	10,039	9.946 ± 2.898	20.138 ± 3.835	100	100	100	Decrease	51	3.6E-10
	10,803	3.338 ± 2.759	17.211 ± 5.869	92	93	93	Decrease	81	1.6E-9
	11,077	4.248 ± 1.608	17.425 ± 4.453	100	100	100	Decrease	76	2.9E-10

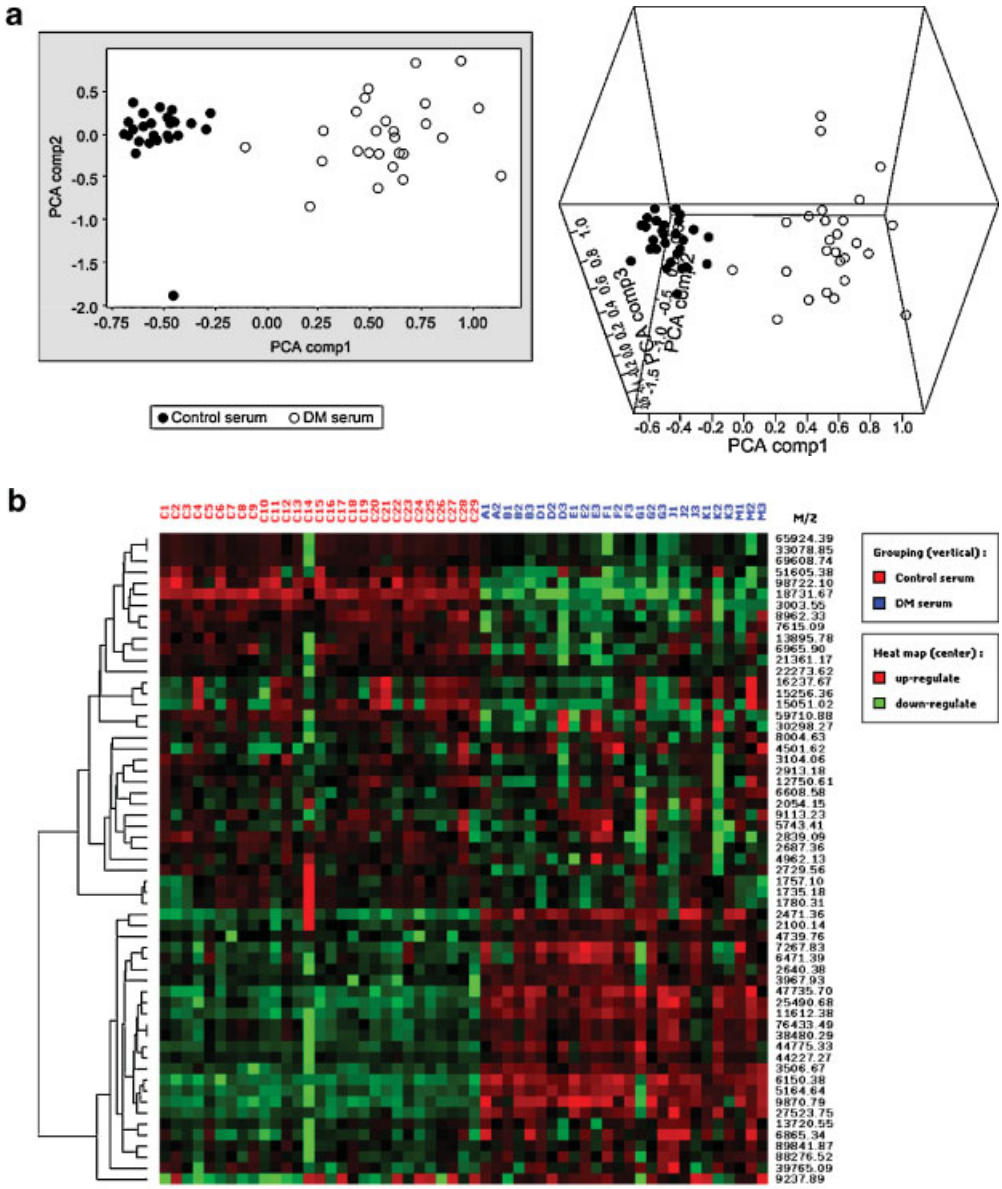

Fig. 1. Protein expression patterns between the 26 diabetes sera and 29 normal control sera. **a**: Principal components analysis of proteome data of diabetes serum and normal control serum represented in a 2D-graph and 3D-graph with components 1–2 and 1–3 displayed on the two axes and three axes. **b**: Heat map presentation of a hierarchical cluster representing similarities in the expression patterns between the diabetes sera (in blue) and normal control sera (in red). The intensity of the red or green color indicates the relative protein concentration, that is, higher than or lower than the median value, respectively.

MW matching identification was conducted as speculative at this stage. One of the serum biomarker candidates at MW 25,491 Da was found to match the CRP in the Swiss-Prot knowledgebase (accession number P48199; MW 25,468 Da; pI 5; MW ranges 0.09%, more stringent than the standard error 0.1% of the current MS analysis). Search by molecular size and pI using the TagIdent tool returned a fragment of CRP at MW 23,285 Da which was found to match another significant peaks cluster at MW 23,306 Da (0.409 ± 0.092 vs. 0.250 ± 0.062, $P = 2.7\text{E-}8$).

The preliminary identification of the tentative biomarker was further validated by established assay. The quantitative measurement of CRP in serum was performed using a commercial ELISA kit to validate the matched protein, and the results were expressed as arithmetic mean $\pm$ SE. As shown in Figure 2, CRP levels of

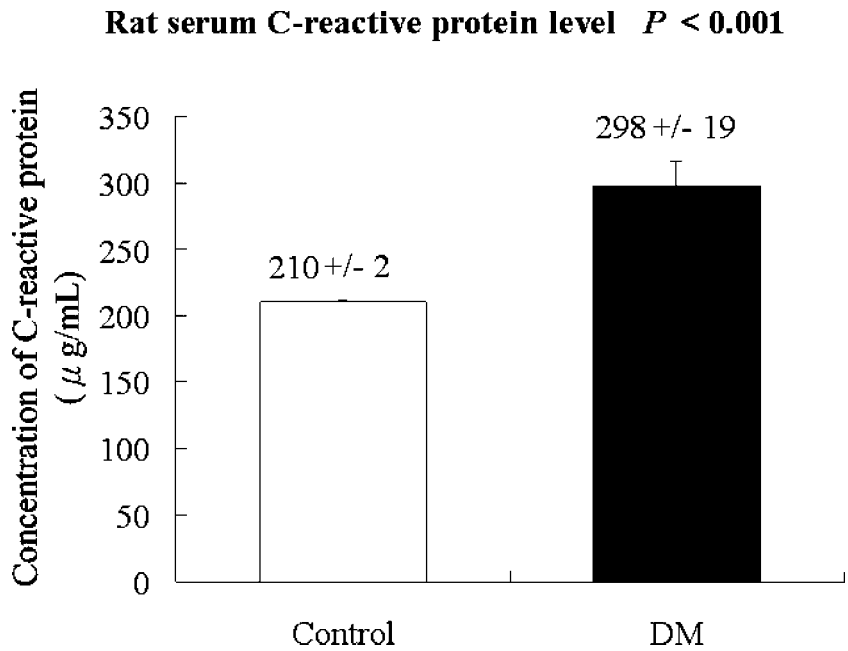

Fig. 2. The levels of C-reactive protein (CRP) on diabetic rats and normal control rats measured by ELISA kit. The mean CRP concentration of diabetic rats is significantly ($P < 0.001$) higher than those of the normal control rats. The normal control rats are marked by (□) and diabetic rats are the (■) box.

the diabetic rats sera (n = 26) were significantly higher than those of the normal controls (n = 29) by 42% (298 ± 19 μg/ml vs. 210 ± 2 μg/ml, $P < 0.001$).

Differential Renal Protein Expression in Diabetic Rats

Comparing the kidney lysate of the DM group with the non-DM group, 81 peak clusters were discovered, of which 23 potential biomarkers were deemed statistically significant ($P < 0.05$). The top biomarker candidate at 13,983 Da was elevated by 99% in the DM group and a 92% sensitivity and 93% specificity were yielded (Table I). The peak of interest of the biomarker candidate was illustrated in Figure 3.

Changes in Protein Expression Between the Eyes of Diabetic Rats and Normal Controls

Biomarkers in the eyes were subsequently investigated. Overall, 218 peak clusters were discovered, among which 70 have a significant *P*-value. Significant alterations of the peak intensities of the top biomarker candidate at 5,621 Da was observed, with a decrease of 61% in its average peak intensity in the diabetic lysate compared to the control lysate (Table I and Fig. 4).

Proteomic Alterations in the Aorta Lysate of Diabetic Rats

A total of 117 peak clusters were found in the profiles of the aorta lysate, of which 62 have a significant *P*-value. The average peak intensities of the top three biomarker candidates at 10,039, 10,803, and 11,077 Da in the diabetic aorta lysate were significantly decreased by 51%, 81%, and 76% compared to the control lysate (Table I and Fig. 5).

DISCUSSSION

General awareness of the importance of proteomes in physiology and pathophysiology has increased tremendously over the last few years [Schulte et al., 2005]. Proteins are involved in most cellular processes, and it is thus expected that their cumulative expression profile reflects the specific activity of cells.

Typically, proteomic information is gathered by analyzing samples on two-dimensional gel electrophoresis with the subsequent identification of specific proteins of interest by using trypsin digestion and peptide mass fingerprinting. These procedures are generally labor-intensive and manual, and therefore of low-throughput. The development of automated

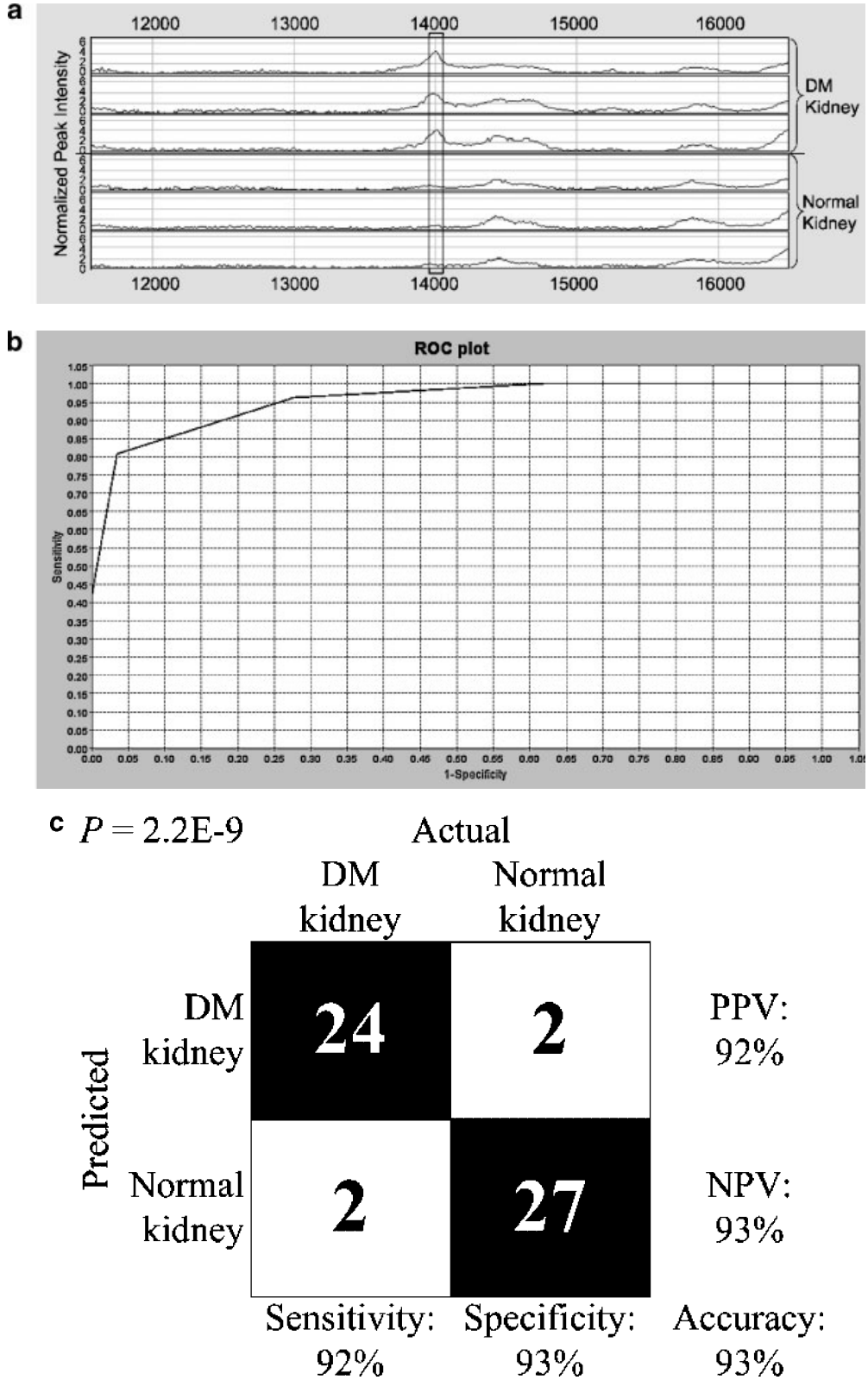

Fig. 3. The detection of potential biomarker at MW 13,983 Da in the kidney tissue of diabetic rat by proteinchip profiling. **a**: Peak views of the mass spectra of kidney lysate samples illustrating the higher intensities of the biomarker candidate in the kidney tissue of diabetic rats compared with normal control rats. **b**: Receiver-operator characteristic curve analysis of the diagnostic score in discriminating between diabetic kidney and normal kidney lysates. **c**: Results of diagnostic testing with 92% sensitivity, 93% specificity, and 93% classification accuracy: PPV = positive predictive value; NPV = negative predictive value.

proteomic technology for processing large numbers of samples simultaneously has made the concept of profiling entire proteomes feasible at last [Lopez et al., 2000].

Proteomics can be useful in describing the protein expression profile and thus the diabetic phenotype. However, relatively few studies using proteomic technologies to investigate the DM pathogenesis have been published to date regarding the defined target organ, the beta-cell. Proteomics has been applied in studies of differentiating beta-cells, cytokine exposed islets, dietary manipulated islets, and in transplanted islets. Although these studies have revealed a complex and detailed picture of the protein expression profiles, many functional implications still remain to be answered [Sparre et al., 2005].

In order to explore the mechanism underlying the development of diabetes and its complications, the serum and lysate protein profiles of STZ-induced diabetic rats were investigated using SELDI-TOF MS in this study. The investigation produced a list of potential biomarkers that were found to be differentially expressed in the serum and selected organs of the diabetic rats 8 weeks after STZ administration.

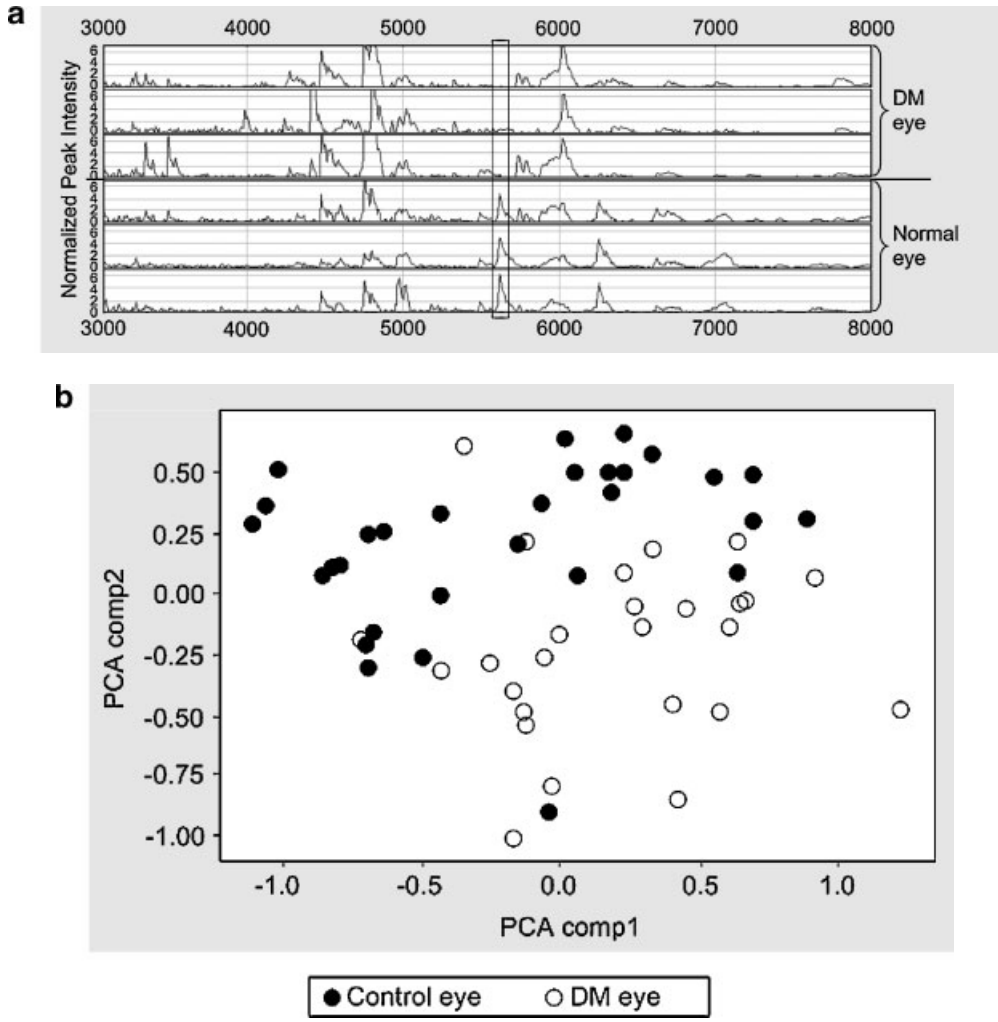

Fig. 4. The detection of potential biomarker at MW 5,621 Da in the eye lysate of diabetic rat by proteinchip profiling. **a**: Peak views of the mass spectra of eye lysate samples illustrating the higher normalized peak intensities of the biomarker candidate in the eye tissue of diabetic rats compared with normal control rats. **b**: Principal components analysis of proteome data of diabetic eye lysate and normal control eye lysate represented in a 2D-graph with components 1–2 displayed on the two axes. **c**: Box and Whisker plot displayed a statistical summary of the normalized peak intensities of the biomarker candidate in the eye tissue of diabetic rats compared with normal control rats: median, quartiles (25–75 percentile) and range (minimum to maximum value).

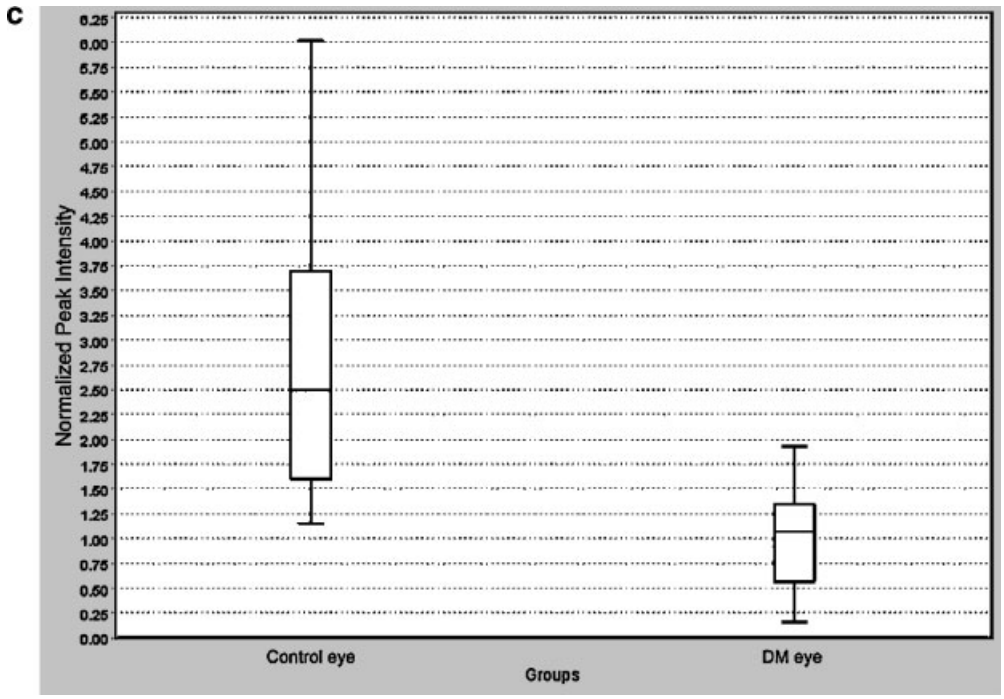

Fig. 4. (*Continued*)

The levels of the eight serum biomarker candidates were significantly elevated in the diabetic state. Identification and characterization of these overexpressed peaks may contribute to a better understanding of the pathogenesis of the disease.

One of the potential serum biomarkers was found to match the CRP in the Swiss-Prot knowledgebase. CRP is produced by the liver in response to inflammation, it is one of the principal members of the pentaxin family. Pentaxins are a family of penta- or decameric serum proteins that includes serum amyloid protein and CRP which are involved in acute immunological responses [Reid and Blobel, 1994].

C-reactive protein is expressed during acute phase response to tissue injury or inflammation in mammals [Romero et al., 1998]. Inflammation is closely associated with endothelial dysfunction and is recognized as one of the cardiovascular risk factors clustering in the insulin resistance syndrome or metabolic syndrome.

In the present study, a significant elevation was observed in the normalized peak intensities of CRP in the diabetic rats. Other previous studies also found that elevated serum CRP level was related to the development of diabetes [Chase et al., 2004; Doi et al., 2005] and its complications, including diabetic atherosclerosis [Tajiri et al., 2005] and cardiovascular complication [Best et al., 2005]. The increased level of CRP in diabetic serum indicates that the development of DM is associated with inflammation.

Further validation was conducted by a commercial ELISA kit to confirm the role of CRP during the development of DM. The CRP levels of the diabetic rats were found to be significantly higher than those of the normal controls. These results are concurrent with our findings by proteinchip profiling.

The metabolic abnormalities associated with DM could lead to a series of microvascular and macrovascular complications in multiple organ systems. The risk for mortality increases with the severity of each complication. Prevention of these complications should be the main issue for managing diabetes. In this study, three vital organs were investigated by proteinchip profiling to probe into the protein alterations in their tissues. Interestingly, compared to the kidney and the aorta, the serum and the eye yielded larger numbers of peak clusters, presumably due to their more aqueous nature.

Despite significant progress in understanding DN, the cellular mechanisms that lead to

diabetes-induced renal damage are still incompletely defined. New insights into the pathogenesis of diabetic renal disease may emerge from recent advances in proteomics using high-throughput mass spectrometry. In our results, the level of the kidney lysate biomarker candidate at 13,983 Da was significantly increased in rats with diabetes over the normal controls. The level of this potential biomarker was positively correlated with the development of DM, it is

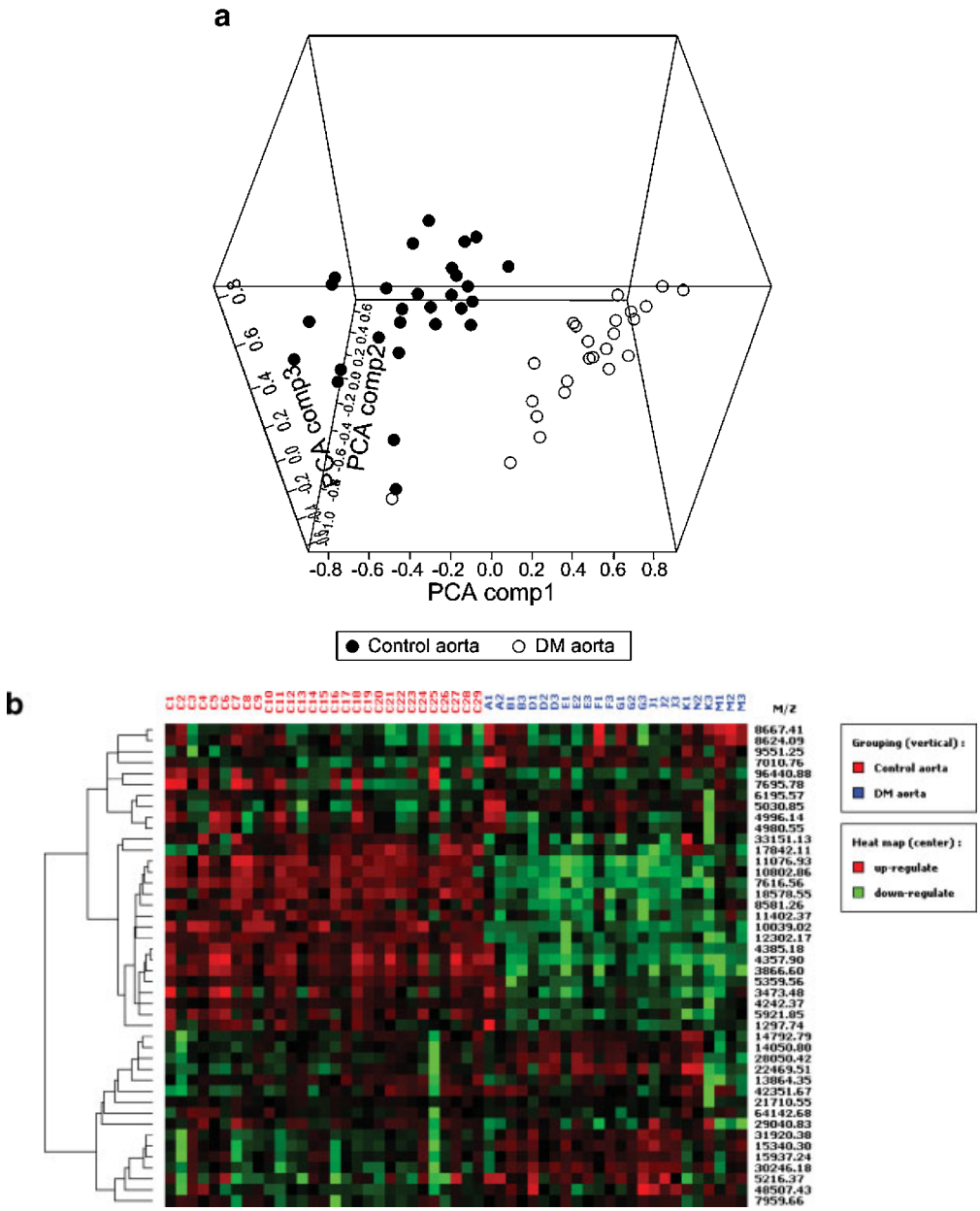

Fig. 5. The detection of potential biomarkers at MW 10,039, 10,803, and 11,077 Da in the aorta lysate of diabetic rat by proteinchip profiling. **a**: Principal components analysis of proteome data of diabetic aorta lysate and normal control aorta lysate represented in a 3D-graph with components 1–3 displayed on the three axes. **b**: Heat map presentation of a hierarchical cluster representing similarities in the expression patterns between the diabetic aorta lysate (in blue) and normal control aorta lysate (in red). The intensity of the red or green color indicates the relative protein concentration, that is, higher than or lower than the median value, respectively. **c**: Distribution of the normalized peak intensities of the three biomarker candidates in diabetic aorta lysate and normal control aorta lysate. Mean peak intensities (±SD) are tabulated at the top of each column. Statistical comparisons of the mean normalized peak intensities in different groups were performed by Mann–Whitney *U* test and presented at the top right corner.

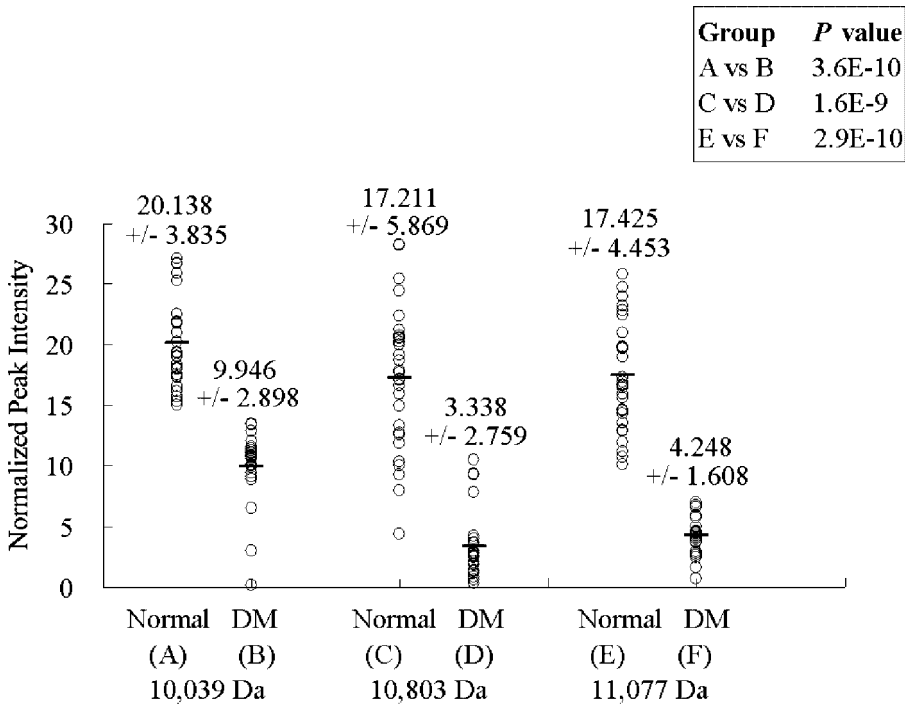

Fig. 5. (*Continued*)

logical to suggest that this biomarker candidate could be associated with DN. It would be interesting to monitor the level of this potential biomarker serially and correlate its level with the extent of renal damage to investigate its role as a surrogate marker for DN.

Recent finding indicates that DR has characteristics of chronic inflammatory disease and neurodegenerative disease [Leal et al., 2005]. Our finding demonstrated that a potential biomarker at 5,621 Da was significantly decreased in the diabetic lysate of the eye compared to the normal controls. Identification and evaluation of this biomarker candidate will enlighten our understanding of the cellular and possibly the molecular mechanisms underlying the pathogenesis of this diabetic complication. This will facilitate the development of strategies to prevent, or at least delay the progression of the disease.

Chronic hyperglycemia induces endothelial dysfunction, which is an early sign of the development of diabetic vascular complications. It is imperative for early detection of cardiac abnormalities during the course of diabetes. Proteomics has been successfully applied to study protein alterations in the vasculature [Mayr et al., 2004]. In this study, three potential biomarkers (10,039, 10,803, and 11,077 Da) identified in the aorta lysate samples of the diabetic rats were significantly decreased as compared with those of the normal controls. Reduced level of these biomarker candidates could be significant indicators for susceptibility to vascular complications in diabetic subjects.

Remarkable applications of proteomics promise a bright future for molecular biology and hopefully for clinical biochemistry. This is the first report demonstrating that certain potential biomarkers in the serum, kidney, eye, and aorta may be involved in the development of diabetes and its complications. In the coming decades, proteomic technologies will broaden our understanding of the underlying mechanisms of DM and will further enhance our ability to diagnose, prognosticate and treat diabetes and its complications.

REFERENCES

Arulmozhi DK, Veeranjaneyulu A, Bodhankar SL. 2004. Neonatal streptozotocin-induced rat model of type 2 diabetes mellitus: A glance. Indian J Pharmacol 36: 217–221.

Best LG, Zhang Y, Lee ET, Yeh JL, Cowan L, Palmieri V, Roman M, Devereux RB, Fabsitz RR, Tracy RP, Robbins D, Davidson M, Ahmed A, Howard BV. 2005. C-reactive

protein as a predictor of cardiovascular risk in a population with a high prevalence of diabetes: The Strong Heart Study. Circulation 112:1289–1295.

Chase HP, Cooper S, Osberg I, Stene LC, Barriga K, Norris J, Eisenbarth GS, Rewers M. 2004. Elevated C-reactive protein levels in the development of type 1 diabetes. Diabetes 53:2569–2573.

Cho WC, Yip TT, Yip C, Yip V, Thulasiraman V, Ngan RK, Yip TT, Lau WH, Au JS, Law SC, Cheng WW, Ma VW, Lim CK. 2004. Identification of serum amyloid A protein as a potentially useful biomarker to monitor relapse of nasopharyngeal cancer by serum proteomic profiling. Clin Cancer Res 10:43–52.

Cho WC, Yue KK, Leung AW. 2005. Proteomics—leading the postgenome era. China Biotechnol 25:33–38.

Doi Y, Kiyohara Y, Kubo M, Ninomiya T, Wakugawa Y, Yonemoto K, Iwase M, Iida M. 2005. Elevated C-reactive protein is a predictor of the development of diabetes in a general Japanese population: The Hisayama Study. Diabetes Care 28:2497–2500.

Gribonval R. 2005. From projection pursuit and CART to adaptive discriminator analysis? IEEE Trans Neural Netw 16:522–532.

Hanson RL, Imperatore G, Bennett PH, Knowler WC. 2002. Components of the "metabolic syndrome" and incidence of type 2 diabetes. Diabetes 51:3120–3127.

Hong H, Dragan Y, Epstein J, Teitel C, Chen B, Xie Q, Fang H, Shi L, Perkins R, Tong W. 2005. Quality control and quality assessment of data from surface-enhanced laser desorption/ionization (SELDI) time-of flight (TOF) mass spectrometry (MS). BMC Bioinformatics 6:S5.

Jayakar SD. 1980. A principal component analysis of quantitative serum protein data. Ric Clin Lab 10:243–246.

Leal EC, Santiago AR, Ambrosio AF. 2005. Old and new drug targets in diabetic retinopathy: From biochemical changes to inflammation and neurodegeneration. Curr Drug Targets CNS Neurol Disord 4:421–434.

Lewis EJ, Lewis JB. 2003. Treatment of diabetic nephropathy with angiotensin II receptor antagonist. Clin Exp Nephrol 7:1–8.

Lopez MF, Kristal BS, Chernokalskaya E, Lazarev A, Shestopalov AI, Bogdanova A, Robinson M. 2000. High-throughput profiling of the mitochondrial proteome using affinity fractionation and automation. Electrophoresis 21:3427–3440.

Mayr M, Mayr U, Chung YL, Yin X, Griffiths JR, Xu Q. 2004. Vascular proteomics: Linking proteomic and metabolomic changes. Proteomics 4:3751–3761.

Nettleman MD. 1988. Receiver operator characteristic (ROC) curves. Infect Control Hosp Epidemiol 9:374–377.

Phillips CA, Molitch ME. 2002. The relationship between glucose control and the development and progression of diabetic nephropathy. Curr Diabetes Rep 2:523–529.

Reid MS, Blobel CP. 1994. Apexin, an acrosomal pentaxin. J Biol Chem 269:32615–32620.

Roglic G, Unwin N, Bennett PH, Mathers C, Tuomilehto J, Nag S, Connolly V, King H. 2005. The burden of mortality attributable to diabetes: Realistic estimates for the year 2000. Diabetes Care 28:2130–2135.

Romero IR, Morris C, Rodriguez M, Du Clos TW, Mold C. 1998. Inflammatory potential of C-reactive protein complexes compared to immune complexes. Clin Immunol Immunopathol 87:155–162.

Schulte I, Tammen H, Selle H, Schulz-Knappe P. 2005. Peptides in body fluids and tissues as markers of disease. Expert Rev Mol Diagn 5:145–157.

Sparre T, Larsen MR, Heding PE, Karlsen AE, Jensen ON, Pociot F. 2005. Unraveling the pathogenesis of type 1 diabetes with proteomics: Present and future directions. Mol Cell Proteomics 4:441–457.

Tajiri Y, Mimura K, Umeda F. 2005. High-sensitivity C-reactive protein in Japanese patients with type 2 diabetes. High-sensitivity C-reactive protein in Japanese patients with type 2 diabetes. Obes Res 13:1810–1816.

Tewari HK, Venkatesh P. 2004. Diabetic retinopathy for general practitioners. J Indian Med Assoc 102:720, 722–723.

Varughese GI, Tomson J, Lip GY. 2005. Type 2 diabetes mellitus: A cardiovascular perspective. Int J Clin Pract 59:798–816.

Whitney J. 1997. Testing for differences with the nonparametric Mann-Whitney *U* test. J Wound Ostomy Continence Nurs 24:12.

Yip TT, Lomas L. 2002. SELDI proteinchip array in oncoproteomic research. Technol Cancer Res Treat 1:273–280.

Yip TT, Chan JW, Cho WC, Yip TT, Wang Z, Kwan TL, Law SC, Tsang DN, Chan JK, Lee KC, Cheng WW, Ma VW, Yip C, Lim CK, Ngan RK, Au JS, Chan A, Lim WW. 2005. Protein chip array profiling analysis in patients with severe acute respiratory syndrome identified serum amyloid A protein as a biomarker potentially useful in monitoring the extent of pneumonia. Clin Chem 51:47–55.

Yue KK, Chung WS, Leung AW, Cheng CH. 2003. Redox changes precede the occurrence of oxidative stress in eyes and aorta, but not in kidneys of diabetic rats. Life Sci 73:2557–2570.

Yue KK, Leung SN, Man PM, Yeung WF, Chung WS, Lee KW, Leung AW, Cheng CH. 2005. Alterations in antioxidant enzyme activities in the eyes, aorta and kidneys of diabetic rats relevant to the onset of oxidative stress. Life Sci 77:721–734.